Bilateral lesions of the mesencephalic trigeminal sensory nucleus stimulate hippocampal neurogenesis but lead to severe deficits in spatial memory resetting

Toshiaki Ishii*, Ryuta Suenaga, Wataru Iwata, Ryouhei Miyata, Ryu Fujikawa, and Yoshikage Muroi

Department of Basic Veterinary Medicine,
Obihiro University of Agriculture and Veterinary Medicine,
Obihiro, Hokkaido 080-8555, Japan

*Correspondence (to):
Dr. Toshiaki Ishii
Department of Basic Veterinary Medicine,
Obihiro University of Agriculture and Veterinary Medicine,
Obihiro, Hokkaido 080-8555, Japan
Tel: +81-155-49-5366, Fax: +81-155-49-5366,
E-mail: ishii@obihiro.ac.jp

Abbreviations

Me5**,** mesencephalic trigeminal nucleus; DG, dentate gyrus; VMH, ventromedial hypothalamus; NeuN, neuronal nuclei; GFAP, glial fibrillary acidic protein; BrdU, 5-bromo-2’-deoxyuridine.

Abstract

The mesencephalic trigeminal sensory nucleus (Me5), which receives signals originating from oral proprioceptors, becomes active at weaning and contributes to the acquisition of active exploratory behavior [Ishii, T., Furuoka, H., Kitamura, N., Muroi, Y., and Nishimura, M. (2006) Brain Res. 1111, 153-161]. Because cognitive functions play a key role in animal exploration, in the present study we assessed the role of Me5 in spatial learning and memory in the water maze. Mice with bilateral Me5 lesions exhibited severe deficits in both a reversal learning and a reversal probe test compared with sham-operated mice. In spite of these reversal tests, Me5 lesions had no effect on a hidden platform test. These results suggest that Me5-lesioned mice show a perseveration of the previously learned spatial strategy rather than an inability to learn a new strategy, resulting in reduced spatial memory resetting. Moreover, adult neurogenesis in the dentate gyrus of the hippocampus, which has been proposed to have a causal relationship to spatial memory, was stimulated in Me5-lesioned mice. Thus, a stimulation of hippocampal neurogenesis observed after Me5 lesions may lead to a rigidity and perseverance of the previously learned strategy because of inferential overuse of past memories in a novel situation. These results suggest that Me5 contributes to spatial memory resetting by controlling the rate of hippocampal neurogenesis through an ascending neuronal pathway to the hippocampus.

Section: Cognitive and Behavioral Neuroscience

Keywords: spatial learning and memory, Me5 lesions, hippocampal neurogenesis, dentate gyrus.

1. Introduction

The mesencephalic trigeminal nucleus (Me5) receives proprioceptive sensory afferents of the trigeminal nerve from the jaw-closing muscle spindles and the periodontal ligaments, and also innervates the motor trigeminal nucleus, relating to the jaw-jerk reflex (Corbin and Haeeison, 1940; Harrison and Corbin, 1942). Me5 fibers project to the tuberomammillary nucleus (TMN) of the posterior hypothalamus (Ericson et al., 1989) while the neurons in the TMN project to the ventromedial hypothalamus (VMH) and also to the Me5 (Inagaki et al., 1987; Inagaki et al., 1988; Sakata et al., 2003). Through the above pathways, the Me5 receives signals relating to mastication-induced proprioceptive sensation and modulates satiation via a satiety center in the VMH (Fujise et al., 1993, 1998).

As a further step to understanding how the Me5 is involved in the control of feeding and exploratory behavior, we previously examined the effect of bilateral electrolytic lesions of the Me5 on these behaviors (Ishii et al., 2005a, 2006). Analysis using a food-search-compulsion-apparatus revealed that Me5 lesions markedly inhibited active exploratory behavior, manifested as low-frequency exploration, and changed feeding profiles such as the number of accessions and the duration of feeding without modulating the emotional state (Ishii et al., 2005a). Moreover, the same low-frequency exploration was observed in mice fed exclusively milk after weaning until 10 weeks of age, and this low-frequency exploration was switched to high-frequency exploration after a switch from exclusively milk formula to a food pellet diet (Ishii et al., 2005b, 2006). However, Me5 lesions prevented the acquisition of this active exploratory behavior (Ishii et al., 2006). Thus, the Me5 is involved in acquisition and maintenance of the active exploratory behavior in mice post weaning (Ishii et al., 2005a, 2005b, 2006).

Animals' propensity for explanation is positively correlated with general learning abilities (Matzel et al., 2003). Moreover, Matzel et al. (2006) found that animals' exploration co-varies with general learning abilities. Recently, Saab et al. (2009) demonstrated that a mouse line with selective manipulation to the dentate gyrus (DG) neurons promotes exploratory behavior and enhances hippocampal synaptic plasticity and rapid acquisition of spatial memory. Although the molecular underpinnings of exploration and its link to learning and memory remain poorly understood, the remarkable plasticity of the hippocampal network has been suggested to underline several neural processes including new acquisition of spatial memory (Goodrich-Hunsaker et al., 2008) and novelty exploration (Lever et al., 2006). Thus, hippocampal functions, such as spatial learning and memory, seem to be implicated in animal exploration. We have previously found that a change of explanation habit from high-frequency to low-frequency after Me5 lesions is irreversible and that this low-frequency exploratory behavior maintains (Ishii et al., 2005a, 2006). Therefore, we hypothesized that the hippocampal functions, such as spatial learning and memory, may be affected in mice with bilateral Me5 lesions.

It is widely accepted that the hippocampus plays a key role in the formation and retrieval of spatial memories. Recent behavioral studies involving discrete lesions of specific hippocampal sectors, including selective lesions of DG, CA3 or CA1, have successfully identified some functional dissociation of each of these areas (Gilbert et al., 2001; Lee and Kesner, 2004; Lee, 2005). Moreover, current computational models are consistent with the notion of functional heterogeneity within the hippocampus (Becker, 2005). It is of interest to investigate whether the Me5, which controls acquisition and maintenance of active exploratory behavior, is indeed relevant to spatial learning and/or memory and, if so, which hippocampal regions are receiving afferent neural signals from the Me5.

The DG is one of the few regions of the mammalian brain where new neurons are generated throughout adulthood (Abrous et al., 2005). These adult-generated granule neurons are integrated into the hippocampal circuitry and exhibit electrophysiological properties similar to those of mature granule neurons (Laplagne et al., 2006), and the recruitment of these new neurons into functional hippocampal networks contributes to updating and strengthening of spatial memory (Trouche et al., 2009). On the other hand, conditions that improve learning abilities in the water maze, such as enriched environments, enhance hippocampal neurogenesis (Kempermann et al., 1997). In contrast, conditions that impair spatial learning, such as prenatal stress, decrease neurogenesis (Lemaire et al., 2000). Moreover, spatial learning associated with water maze training enhances adult neurogenesis (Gould et al., 1999) and promotes survival of new neurons in the DG (Trouche et al., 2009). Thus, it seems that spatial memory and hippocampal adult neurogenesis correlate to each other. Exploration gives a lot of spatial cues necessary for the encoding and the use of a spatial map, and spatial relational memory is established in association with these multiple spatial cues. Because Me5 lesions markedly inhibited active exploratory behavior, it is important to examine the effects of Me5 lesions on hippocampal neurogenesis and spatial learning and/or memory.

In the present study, we examined whether bilateral Me5 lesions influence hippocampal formation and spatial learning and/or memory. Our results indicate that bilateral Me5 lesions stimulate hippocampal neurogenesis but lead to severe deficits in spatial memory resetting.

2. Results

2.1. General behavioral activities in the automated hole-board test

Prior to the Morris water maze task, we examined general behavioral activities in both Me5-lesioned and sham-operated mice using an automated hole-board. No significant

differences in general behavioral activities between those mice were observed (Table 1). These results suggest that Me5 lesions do not influence spontaneous activities of mice, confirming results obtained in our previous study (Ishii et al., 2005a).

2.2. Me5 lesions are specifically associated with memory impairments in the reversal platform version of the Morris water maze

We tested spatial learning in Me5-lesioned and sham-operated mice using the hidden-platform version of the Morris water maze, a hippocampus-dependent learning task (Schenk and Morris, 1985). During training for this task, mice learn to locate a hidden platform using distal environmental cues. We trained bilaterally Me5-lesioned and sham-operated mice with four trials per day for 5 consecutive days. The two groups showed significant improvement in mean latency during trails (sham-operated mice: Friedman test, $p < 0.01$; Dunnett *post hoc* comparisons with escape latency: $^{+}p < 0.05$ and $*p < 0.01$ vs. the first day. Me5-lesioned mice: one-way repeated-measures ANOVA, $F(4, 55) = 14.786$, $p < 0.01$; Tukey-Kramer test *post hoc* comparisons with escape latency, $^{+}p < 0.05$ and $*p < 0.01$ vs. the first day) (Fig. 1A). However, there was no significant difference between the groups.

The normal acquisition of spatial memory by both groups was further demonstrated by their performance in the probe test (Fig. 1B), in which all mice spent significantly more time in the trained quadrant (target quadrant) than in the other two or three quadrants (sham-operated mice: one-way repeated-measures ANOVA, $F(3, 28) = 14.791$, $p < 0.01$; Tukey-Kramer test *post hoc* comparisons with time spent in target quadrant, $p < 0.01$ for left quadrant, $p < 0.05$ for right quadrant, $p < 0.01$ for opposite quadrant. Me5-lesioned mice: one-way repeated-measures ANOVA, $F(3, 44) = 12.525$, $p < 0.01$; Tukey-Kramer test *post hoc* comparisons with time

spent in target quadrant, $p < 0.01$ for left quadrant, $p = 0.11$ for right quadrant, $p < 0.01$ for opposite quadrant).

Next, we examined Me5-lesioned and sham-operated mice in reversal learning and reversal probe tests using the reversal platform version of the Morris water maze task, in which the previous position of the hidden platform was switched to the opposite quadrant for training. Sham-operated mice showed significant improvement in mean latency during the 2 days of reversal training (paired *t* test, $^{a}p < 0.01$) and were judged to have learned the new position of the reversal platform by day 2 based on a decrease in the latency of reaching the platform to < 40 s (Fig. 2A). However, bilateral Me5-lesioned mice did not show significant improvement in mean latency (paired *t* test, p = 0.19) and had significantly longer latencies on the day 2 of reversal training than sham-operated mice (Welch's *t* test, $^{b}p < 0.01$). Deficits in the performance of the bilateral Me5-lesioned mice were also found in the reversal probe test following reversal training; the bilateral Me5-lesioned mice spent more time in the previous target quadrant than the new target quadrant (Fig. 2B) (Me5-lesioned mice: one-way repeated-measures ANOVA, $F(3, 44) = 3.785$, $p < 0.05$; Tukey-Kramer *post hoc* comparisons with time spent in the new target quadrant, $p < 0.05$ for the previous target quadrant, $p = 0.98$ for left quadrant, $p = 0.62$ for right quadrant). Conversely, sham-operated mice spent more time in the new target quadrant than in the previous target quadrant (Fig. 2B) (sham-operated mice: one-way repeated-measures ANOVA, $F(3, 28) = 10.877$, $p < 0.01$; Tukey-Kramer *post hoc* comparisons with time spent in the new target quadrant, $p < 0.01$ for the previous target quadrant, $p < 0.01$ for left quadrant, $p = 0.41$ for right quadrant). Thus, bilateral Me5-lesioned mice showed a preference for the previous target quadrant over the new target quadrant.

We also tested Me5-lesioned and sham-operated mice in the visible platform version of the Morris water maze, in which mice learned the location of a platform marked with a visible

cue. Sham-operated but not Me5-lesioned mice showed significant improvement in mean latency during the 2 days of visible platform training (Wilcoxon signed-ranks test, $^{a}p < 0.01$ vs. the first day for sham-operated mice; paired *t* test, p = 0.06 vs. the first day for Me5-lesioned mice), and there was a significant difference between the groups (Student's *t* test, $^{b}p < 0.01$ on day 2) (Fig. 3). This slower learning observed in the Me5-lesioned mice might reflect a motivational defect instead of visual deficits because there was no significant difference in the hidden-platform test between the groups.

2.3. Me5 lesions increase cell proliferation in the dentate gyrus

We examined the effect of bilateral Me5 lesions on new cell proliferation in the dentate gyrus (DG). Bilateral electrolytic Me5 lesions were made in 6-wk-old mice, and cell proliferation was assessed by administration of bromodeoxyuridine (BrdU; 100 mg/kg, twice a day for 3 days) 2 wks after lesioning. BrdU-labeled cells analyzed 24 hrs after administration were distributed in the inner layer of the granular cell layer and the hilus of the DG (Fig.4A). The total number of BrdU-labeled cells in Me5-lesioned mice was significantly higher than that in sham-operated mice analyzed in the whole DG (Student's *t* test, *p < 0.05 (Fig.4B). Moreover, the same results were obtained by image analysis in the part of the DG via confocal laser scanning microscopy (Fig. 5B left and 6B left). The extent of differentiation of BrdU-labeled cells was determined by double labeling immunohistochemistry with antibodies against BrdU and the neuronal maker neuron-specific marker (NeuN) or the glial marker, glial fibrillary acidic protein (GFAP). Analysis of colocalization of BrdU with NeuN or GFAP using confocal laser scanning microscopy indicated that the majority of BrdU-labeled cells in sham-operated mice had the neuronal phenotype (~55%) and that a low percentage of BrdU-labeled cells were labeled for GFAP (~29%) (Fig. 5B and 6B). In Me5-lesioned mice compared to sham-operated

mice, the percentage of cells double labeled with BrdU and NeuN was significantly increased (Student's *t* test, $^{b,c}p < 0.01$) (Fig. 5B) but that of cells double labeled with BrdU and GFAP was significantly decreased (Student's *t* test, $^{b}p < 0.05$) (Fig. 6B right), suggesting that the majority of the increased number of BrdU-labeled cells in Me5-lesioned mice possessed the neuronal phenotype.

3. Discussion

It has been reported that general learning ability correlates positively with exploratory behavior in mice (Matzel et al., 2006) and several hypotheses have been proposed to account for this relationship (Matzel et al., 2003). Recently, we have found that the Me5 is involved in acquisition and maintenance of active exploratory behavior in mice post weaning (Ishii et al., 2005a, 2005b, 2006). Therefore, we examined whether bilateral Me5 lesions affect hippocampal formation and spatial learning and/or memory in mice. In the present study, we demonstrated that the Me5 negatively controls neurogenesis in the hippocampal DG and facilitates resetting of spatial memory in response to novel but similar spatial conditions to those previously experienced, possibly through its ascending neuronal pathway to the hippocampus.

We first tested Me5-lesioned and sham-operated mice in spatial learning using the hidden-platform version of the Morris water maze. Mice with bilateral Me5 lesions exhibited severe deficits in both reversal learning and reversal probe tests compared with sham-operated mice. Namely, Me5-lesioned mice showed no improvement in mean latency during the 2 days of reversal training and consequently spent more time in the previous target quadrant than in the new target quadrant (Fig. 2), indicating an impaired learning and/or memory for the new target location. The errors in performance by Me5-lesioned mice in the reversal learning test,

the test used to evaluate cognitive flexibility (McAlonan and Brown, 2000; White, 2004; Stack et al., 2008), may have been due to a slower learning process because of the use of a different learning strategy from the previous one in the novel situation. In spite of deficits in reversal tests, Me5 lesions had no effect on a hidden platform test. Me5 lesions appear to be associated with a perseveration of the previously learned strategy rather than the inability to learn a new strategy. On the other hand, bilateral Me5-lesioned mice showed slower learning in the visible platform test compared to sham-operated mice. Although the reasons for the differences between the two groups in the visible platform test remain unknown, the result implies that Me5 lesions may cause motivational deficits that slow down or prevent learning the location of a platform marked with a visible cue because of the use of a different learning strategy from previous maze trials.

It is widely accepted that the hippocampus is a key structure in memory storage and recall; however, increasing evidence suggests that the hippocampus is also involved in novelty detection by comparing previously encountered information with novel information (Lisman and Otmakhova, 2001). The comparison of expectations based on previous experience arising from the CA3 area and novel information arising from the entrorhinal cortex is suggested to take place in the CA1 area (Lisman and Otmakhova, 2001). Thus, the CA1 and CA3 subfields of the hippocampus could play a prominent role in spatial reversal learning. On the other hand, a recent report suggests that the DG is strongly activated during the initial stages of spatial learning (Poirier et al., 2008) in response to novel spatial conditions (Jenkins et al., 2004) and that activation of both CA1 and CA3 occurs at the later stages of spatial learning (Poirier et al., 2008). Hence, it has also been proposed that the DG and its influence on CA3 are more important for the encoding of novel spatial information but not necessarily for retrieval processes, whereas CA3 and especially CA1 are more critical for consolidation or retrieval

processes of previously stored information (Lee and Kesner, 2004; Remondes and Schuman, 2004). Considering these reports, the deficit observed in this study in the performance by Me5-lesioned mice in reversal learning and probe tests might reflect a weakness in DG function.

The DG of the hippocampus is one of the few regions of the mammalian brain where new neurons are generated throughout adulthood (Abrous et al., 2005). Some of these adult-born granule neurons are integrated into the hippocampal circuitry and exhibit electrophysiological properties similar to those of mature granule neurons (Laplagne et al., 2006), raising the possibility that they may thereby contribute to behaviorally relevant hippocampal neuronal function. Supporting this idea, an increasing number of reports indicate the existence of a functional link between hippocampal-dependent learning and adult hippocampal neurogenesis (Trouch et al., 2009; Dupret et al., 2008; Hernandes-Rabaza et al., 2009; Shors et al., 2001; Snyder et al., 127). Therefore, we examined the effect of bilateral Me5 lesions on new cell proliferation in the DG. Surprisingly, although Me5-lesioned mice exhibited severe deficits in both reversal learning and reversal probe tests, Me5 lesions led to an increase in cell proliferation in the DG. Moreover, the percentage of the cells double labeled with BrdU and NeuN but not with BrdU and GFAP was significantly increased in Me5-lesioned mice, indicating that the increased BrdU-labeled cells in Me5-lesioned mice possessed the neuronal phenotype. Thus, Me5 lesions lead to the upregulation of neurogenesis in the DG. These results suggest that the Me5 physiologically controls adult hippocampal neurogenesis. Moreover, the severe deficits in both reversal learning and reversal probe tests suggest that Me5-lesion-induced upregulation of neurogenesis resulted in perseveration of the previously learned strategy and an impaired learning and/or memory for the new target location. It is possible that alteration in cell proliferation and/or neurogenesis in the DG alters the inferential

use of past memories in a novel situation (flexibility) and thus leads to rigidity and perseverance.

We have previously found that Me5 lesions markedly inhibit active exploratory behavior, manifested as low-frequency exploration (Ishii et al., 2005a; 2006). In the present study, we demonstrated that Me5 lesions stimulate hippocampal neurogenesis and lead to a perseveration of the previously learned strategy but not the inability to learn a new strategy. Furthermore, recruitment of adult-generated neurons into functional hippocampal networks contributes to updating and strengthening of a previously encoded spatial memory (Trouche et al., 2009). Therefore, we assume that low-frequency exploration observed in Me5-lesioned mice (Ishii et al., 2005a, 2006), might reflect persistence of the previously learned strategy of exploration and prevent creation of a new strategy of exploration because of weakened motivation to explore a novel environment.

4. Experimental procedures

4.1. Animals

Male *ddY* mice were maintained under controlled temperature and lighting conditions with a 12-h light/12-h dark cycle (lights on at 0600) and allowed *ad libitum* access to food and water. All procedures for the care and use of experimental animals were approved by the Animal Research Committee in Obihiro University of Agriculture and Veterinary Medicine and were conducted under the Guidelines for Animal Experiments in Obihiro University of Agriculture and Veterinary Medicine and the Guiding Principles in the Use of Animals in Toxicology that were adopted by the Society of Toxicology in 1989. The animals were humanely euthanized by an overdose of anesthetic ether at the end of the experiment.

4.2. Me5 lesions

Bilateral electrolytic Me5 lesions were made in 6-wk-old mice anesthetized with Avertin® (0.36 g/kg). Using a stereotaxic apparatus, a 0.2-mm-diameter stainless steel electrode was positioned 5.3 mm posterior to the bregma, 0.9 mm lateral to the midsagittal suture, and 3.2 mm below the surface of the skull. As previously described, anodal electrolytic lesions were produced by passing a 1.3-mA current through the electrode three times for 1 s each (Ishii et al., 2005a). Out of 41 mice that underwent lesioning, 20 had successful bilateral Me5 lesions, 5 had unilateral Me5 lesions, and 16 had lesions in peri-Me5 regions. All successful Me5 lesions were restricted to the caudal level of the Me5. Sham-operated mice (27 mice) underwent an identical operation but without application of a current. After fixation with 4% neutral-buffered paraformaldehyde solution, serial brain sections (40 µm thick) were cut and stained with hematoxylin-eosin or for Nissl substance with a solution of 0.1% Cresyl Echt Violet and 0.04% acetic acid to reveal the extent of damage to the Me5 (Fig. 4C). Only data from the mice with successful Me5 lesions were used.

4.3. General behavioral activity

General behavioral activity was assessed using an automatic hole-board (model ST-1; Muromachi Kikai, Tokyo, Japan) consisting of a gray wooden box (50 x 50 x 50 cm) with four 3 cm equidistant holes in the floor. A wall-mounted infrared beam sensor was used to detect the number and duration of rearing and head-dipping behaviors and latency to first head-dipping. Other behavioral parameters such as locus, distance and speed of movement of mice in the hole-board were recorded by an overhead color CCD camera; the heads of the mice were painted yellow and the color CCD camera followed their center of gravity. Data from the infrared beam sensor and the CCD camera were collected through a custom-designed interface

(CAT-10; Muromachi Kika) as a reflection signal. Head-dipping behaviors were double-checked via an infrared sensor and the overhead color CCD camera. Thus, head-dipping behavior was counted only when both the head intercepted the infrared beam and the head was detected at the hole by the CCD camera. All data were analyzed and stored on a personal computer using analytical software (Comp ACT HBS; Muromachi Kika). Mice were placed in the center of the hole-board and allowed to freely explore the apparatus for 5 min while exploratory activities were automatically recorded.

4.4. Water maze task

The system for the Morris water maze task consists of a round water tank (120 cm in diameter, filled with ~24°C water), a transparent platform (10 cm in diameter), and a computer-based video automated color tracking apparatus (DVTrack, Model DVT-11; Muromachi Kikai) recorded the position of the mouse in the tank. The platform was submerged 0.6 cm below the water surface. Mice were first trained to find the hidden platform and escape onto the platform fixed in the center of one of the four quadrants of the pool for four trials per day with an inter-trial interval of 30 min over 5 consecutive days. The start positions were selected semi-randomly from five of eight equally spaced well locations, excluding the nearest point and the two second nearest points from the platform. The mice were allowed to swim until they mounted the platform and spent 30 s on it before being returned to their home cages. If the mice failed to find to the platform within the 120 s limit, they were placed on the platform for 30 s. A hidden probe test was given 30 min after the last trial on day 5. For this test, the platform was removed from the pool, and the mouse was allowed to swim freely for 60 s. The time spent in each of the quadrants was measured by the automatic tracking system. On day 6, the hidden platform was switched to the opposite quadrant for reversal training. The mice received four

trials on both day 6 and day 7. A reversal probe test was given 30 min after the last trial on day 7. On day 8 and day 9, for a visible platform test, the position of the platform was signaled by the presence of a white flag (8 x 8 cm) above the platform. The platform position varied among four possible positions, and the mice were tested on a total of four trials at an inter-trial interval of 30 min with a different starting point.

4.5. 5-bromo-2'-deoxyuridine (BrdU) immunohistochemistry

Mice were injected with BrdU (100 mg/kg in saline containing 0.007 N NaOH, i.p.) twice a day (0800 and 1700 h) for 3 days. Twelve hours after the last injection, the mice were anesthetized with Avertin® (0.36 g/kg) and transcardially perfused with heparinized PBS, followed by 15 ml of 4% neutral-buffered paraformaldehyde solution. The brains were dissected and post-fixed with 10% neutral-buffered paraformaldehyde solution. This time-course of injection and survival time was chosen based on the results of the change in behavior after weaning (Ishii et al. 2006). Post-fixation, the brains were cut on an oscillating tissue slicer (Linear slicer Pro7; Dosaka, Kyoto, Japan) (40 mm thick sections) throughout the DG and cerebellum. To prepare slices equally among them and also between groups, we carefully set brain tissues horizontally on the cutting stage of the slicer and kept the tissues under the ice-cold condition. For BrdU immunohistochemistry, the sections were permeabilized with 0.5% (v/v) Triton X-100 in phosphate buffered saline (TPBS) for 1 h, incubated with Pronase E (3 μg/ml) in phosphate buffered saline (PBS) at 37°C for 20 min, denatured in 2 N HCl for 10 min, rinsed twice in PBS, blocked in 2.0% normal rabbit serum for 1 h, and incubated for 36 h at 4°C in sheep anti-BrdU polyclonal antibody (Exalpha Biologicals, Boston, MA; final dilution 1:10,000 in TPBS). For stereological analysis of the total number of BrdU-labeled cells in the whole dentate gyrus, the sections were rinsed in TPBS and incubated for 2 h in biotinylated sheep secondary antisera

(Vector Laboratories, Burlingame, CA; 1: 200 in TPBS). After rinsing in TPBS, the sections were incubated for 1 h in avidin-biotin-horseradish peroxidase (Vector Laboratories; 1: 50 in TPBS), rinsed in PBS, and reacted for 10 min in 0.02% diaminobenzidine (DAB) with 0.02% H_2O_2. After rinsing in PBS, the sections were mounted and coverslipped under 50% glycerol in PBS. It has been reported that spatial learning associated with water maze training enhances adult neurogenesis (Gould et al., 1999) and also promotes survival of new neurons (Trouche et al., 2009) in the DG. To avoid these influences on neurogenesis, we examined the effect of Me5 lesions on neurogenesis in mice without being subjected to any of the Morris water maze tasks.

4.6. Fluorescent double-immunocytochemical staining

For double fluorescence immunolabeling to determine the phenotypes of BrdU-labeled cells, brain sections were processed for BrdU and NeuN or GFAP fluorescent double labeling. Briefly, sections were first pretreated for DNA denaturation as described above, and then incubated for 36 h at 4°C in sheep anti-BrdU polyclonal antibody (Exalpha Biologicals; final dilution 1:10,000 in TPBS) and mouse anti- NeuN monoclonal antibody (Millipore, Billerica, MA ; 1:500 in TPBS) or rabbit anti- GFAP polyclonal antibody (DakoCytomation, Tokyo, Japan; 1:100 in TPBS). After rinsing in TPBS, sections were incubated for 24 h with fluorescent secondary antibodies: AlexaFluor® 488 donkey anti-sheep IgG (Invitrogen, Carlsbad, CA; 1:500 in TBST) to reveal the immunoreactivity of BrdU and AlexaFluor® 633 goat anti-mouse IgG (Invitrogen; 1:500 in TBST) or AlexaFluor® 633 goat anti-rabbit IgG (Invitrogen; 1:500 in TBST) to reveal the immunoreactivity of NeuN or GFAP, respectively. The sections were then rinsed in PBS, mounted onto glass slides, and coverslipped with

mounting medium suitable for fluorescence microscopy (Vectashield; Vector laboratories). Images were obtained by confocal laser scanning microscopy (Nikon, Tokyo, Japan).

4.7. Cell quantification and analysis

Stereological analysis was used to estimate the total number of BrdU-labeled cells in the DG using the optical fractionator method (West et al., 1991) on every twelfth section. For each section, the number of BrdU-labeled cells in the DG was determined, avoiding counts of cells in the outermost plane of focus. In the immunofluorescent analysis, single BrdU-labeled cells and double labeled cells for BrdU and NeuN or GFAP were visualized and counted using a confocal laser scanning microscopy with a 40x objective via the optical fractionator technique. The extent of co-localization was further verified by viewing cells on three planes (X, Y, and Z) using Z-plane sectioning as follows: sections (40 μm thick) were optically sliced in the Z plane at a 1-μm interval by using a 60x oil-immersion objective, and labeled cells were rotated in orthogonal planes (X and Y) to verify double labeling. All acquisitions were carried out in sequential scanning mode to prevent cross-bleeding between channels. The number of BrdU-labeled cells that were labeled with NeuN or GFAP was determined by counting these cells in five DG sections (positioned 1.82 – 2.34 mm posterior to the bregma) from each mouse. These sections comprised every third section of a series of 13 sections (40 μm thick sections) from the DG (1.82 – 2.34 mm posterior to bregma). Images were also captured with 20x objective lens on a confocal laser scanning microscope using Nikon software (EZ-C1). The percentage of BrdU cells double labeled for NeuN or GFAP was calculated by dividing the number of double labeled cells by the total number of BrdU cells in each of the five sections sampled, and averaging.

4.8. Statistical methods

Data obtained from the water maze tasks were analyzed by one-way factorial or one-way repeated-measures ANOVA. When a significant interaction was found ($p < 0.05$), *post hoc* analysis was performed. Data between the two groups were analyzed by Student's t test following Levene's test. All statistical analyses were performed using SPSS 16.0 software (SPSS Japan Inc., Tokyo, Japan).

Acknowledgements

This work was supported by: a Grant-in-Aid for Scientific Research (B) (to T.I.) from the Japan Society for the Promotion of Science; and the President's Discretionary Budget of Obihiro University of Agriculture and Veterinary Medicine (to T.I.).

References

Abrous, D.N., Koehi, M., Moal, M.L., 2005. Adult neurogenesis: from precursors to network and physiology. Physiol. Rev. 85, 523-569.

Becker, S., 2005. A computational principle for hippocampal learning and neurogenesis. Hippocampus 15, 722-738.

Corbin, K.B., Harrison, F., 1940. Function of mesencephalic root of fifth cranial nerve. J. Neurophysiol. 3, 423-435.

Dupret, D., Revest, J.M., Koehl, M., Ichas, F., Giorgi, F.D., Costet, P., Abrous, D.N., Piazza, P.V., 2008. Spatial relational memory requires hippocampal adult neurogenesis. PLoS one 3, e1959.

Ericson, H., Blomqvist, A., Kohler, C., 1989. Brainstem afferents to the tuberomammillary nucleus in the rat brain with special reference to monoaminergic innervation. J. Comp. Neurol. 281, 169-192.

Fujise, T., Yoshimatsu, H., Kurokawa, M., Fukagawa, K., Nakata, M., Sakata, T., 1993. Food consistency modulates eating volume and speed through brain histamine in rat. Brain Res. Bull. 32, 555-559.

Fujise, T., Yoshimatsu, H., Kurokawa, M., Oohara, A., Kang, M., Nakata, M., Sakata, T., 1998. Satiation and masticatory function modulated by brain histamine in rats. Proc. Soc. Exp. Biol. Med. 217, 228-234.

Gilbert, P.E., Kesner, R.P., Lee, I., 2001. Dissociating hippocampal subregions:double dissociation between dentate and CA1. Hippocampus 11, 626-636.

Goodrich-Hunsaker, N.J., Hunsaker, M.R., Kesner, R.P., 2008. The interactions and dissociations of the dorsal hippocampus subregions: how the dentate gyrus, CA3, and CA1 process spatial information. Behav. Neurosci. 122, 16-26.

Gould, E., Beylin, A., Tanapat, P., Reeves, A., Shors, T., 1999. Learning enhances adult neurogenesis in the hippocampal formation. Nat. Neurosci. 2, 260-265.

Harrison, F., Corbin, K.B., 1942. The central pathway for the jaw-jerk. Am. J. Physiol. 135, 439-445.

Hernandez-Rabaza, V., Llorens-Martin, M., Velazquez-Sanchez, C., Ferragud, A., Arcusa, A., Gumus, H.G., Gomez-Pinedo, U., Perez-Villalba, A., Rosello, J., Trejo, J.L., Barcia, J.A., Canales, J.J., 2009. Inhibition of adult hippocampal neurogenesis disrupts contextual learning but spares spatial working memory, long-term conditional rule retention and spatial reversal. Neuroscience 159, 59-68.

Inagaki, N., Yamatodani, A., Shinoda, K., Shiotani, Y., Tohyama, M., Watanabe, T., Wada, H., 1987. The histaminergic innervation of the mesencephalic nucleus of the trigeminal nerve in rat brain: a light and electron microscopical study. Brain Res. 418, 388-391.

Inagaki, N., Yamatodani, A., Ando-Yamamoto, M., Tohyama, M., Watanabe, T., Wada, H., 1988. Organization of histaminergic fibers in the rat brain. J. Comp. Neurol. 273, 283-300.

Ishii, T., Furuoka, H., Itou, T., Kitamura, N., Nishimura, M., 2005a. The mesencephalic trigeminal sensory nucleus is involved in the control of feeding and exploratory behavior in mice, Brain Res. 1048, 80-86.

Ishii, T., Itou, T., Nishimura, M., 2005b. Comparison of growth and exploratory behavior in mice fed an exclusively milk formula diet and mice fed a food-pellet diet post weaning. Life Sci. 78, 174-179.

Ishii, T., Furuoka, H., Kitamura, N., Muroi, Y., Nishimura, M., 2006. The mesencephalic trigeminal sensory nucleus is involved in acquisition of active exploratory behavior induced by changing from a diet of exclusively milk formula to food pellets in mice. Brain Res. 1111, 153-161.

Jenkins, T.A., Amin, E., Pearce, J.M., Brawn, M.W., Aggleton, J.P., 2004. Novel spatial arrangements of familiar visual stimuli promote activity in the rat hippocampal formation but not the parahippocampal cortices: a *c-fos* expression study. Neuroscience 124, 43-52.

Kempermann, G., Kuhn, H.G., Gage, F.H., 1997. More hippocampal neurons in adult mice living in an enriched environment. Nature 386, 493-495.

Laplagne, D.A., Esposito, M.S., Piatti, V.C., Morgenstem, N.A., Zhao, C., van Praag, H., Gage, F.H., Schinder, A.F., 2006. Functional convergence of neurons generated in the developing and adult hippocampus. PLoS Biol. 4, e409.

Lee, I., Kesner, R.P., 2004. Encoding versus retrieval of spatial memory: double dissociation between the dentate gyrus and the perforant path into CA3 in the dorsal hippocampus. Hippocampus 14, 66-76.

Lee, I., Hunsaker, M.R., Kesner, R.P., 2005. The role of hippocampal subregions in detecting spatial novelty. Behav. Neurosci. 119, 342-345.

Lemaire, V., Koehl, M., Le Moal, M., Abrous, D.N., 2000. Prenatal stress produces learning deficits associated with an inhibition of neurogenesis in the hippocampus. Proc. Natl. Acad. Sci. USA 97, 11032-11037.

Lever, C., Burton, S., O'Keefe, J., 2006. Rearing on hind legs, environmental novelty, and the hippocampal formation. Rev. Neurosci. 17, 111-133.

Lisman, J.E., Otmakhova, N.A., 2001. Storage, recall, and novelty detection of sequences by the hippocampus: elaborating on the SOCRATIC model to account for normal and aberrant effects of dopamine. Hippocampus 11, 551-568.

Matzel, L.D., Han, Y.R., Grossman, H., Karnik, M.S., Patel, D., Scott, N., Specht, S.M., Gandhi, C.C., 2003. Individual differences in the expression of a "general" learning ability in mice. J. Neurosci. 23, 6423-6433.

Matzel, L.D., Townsend, D.A., Grossman, H., Han, Y.R., Hale, G., Zappulla, M., Light, K., Kolata, S., 2006. Exploration in outbred mice covaries with general learning abilities irrespective of stress reactivity, emotionality, and physical attributes. Neurobiol. Learn. Mem. 86, 228-240.

McAlonan, K., Brown, V.J., 2003. Orbital prefrontal cortex mediates reversal learning and not attentional set shifting in the rat. Behav. Brain Res. 146, 97-103.

Poirier, G.L., Amin, E., Aggleton, J.P., 2008. Qualitatively different hippocampal subfield engagement emerges with mastery of a spatial memory task by rats. J. Neurosci. 28, 1032-1045.

Remondes, M., Schuman, E.M., 2004. Role for a cortical input to hippocampal area CA1 in the consolidation of a long-term memory. Nature 431, 699-703.

Saab, B.J., Georgiou, J., Nath, A., Lee, F.J.S., Wang, M., Michalon, A., Liu, F., Mansuy, I.M., Roder, J.C., 2009. NCS-1 in the dentate gyrus promotes exploration, synaptic plasticity, and rapid acquisition of spatial memory. Neuron 63, 643-656.

Sakata, T., Yoshimatsu, H., Masaki, T., Tsuda, K., 2003. Anti-obesity actions of mastication driven by histamine neurons in rats. Exp. Biol. Med. 228, 1106-1110.

Schenk, F., Morris, R.G.M., 1985. Dissociation between components of spatial memory in rats after recovery from the effects of retrohippocampal lesions. Exp. Brain Res. 58, 11-28.

Shors, T.J., Miesegaes, G., Beylin, A., Zhao, M., Rydel, T., Gould, E., 2001. Neurogenesis in the adult is involved in the formation of trace memories. Nature 410, 372-376.

Stack, C.M., Lim, M.A., Cuasay, K., Stone, M.M., Seibert, K.M., Spivak-Pohis, I., Crawley, J.N., Waschek, J.A., Hill, J.M., 2008. Deficits in social behavior and reversal learning are more prevalent in mice offspring of VIP deficient female mice. Exp. Neurol. 211, 67-84.

Snyder, J.S., Hong, N.S., Mcdonald, R.J., Wojtowicz, J.M., 2005. A role for adult neurogenesis in spatial long-term memory. Neuroscience 130, 843-852.

Trouche, S., Bontempi, B., Roullet, P., Rampon, C., 2009. Recruitment of adult-generated neurons into functional hippocampal networks contributes to updating and strengthening of spatial memory. Proc. Natl. Acad. Sci. USA 106, 5919-5924.

West, M.J., Slomianka, L. & Gundersen, H.J.G., 1991. Unbiased stereological estimation of the total number of neurons in the subdivisions of the rat hippocampus using the optical fractionator. *Anat. Rec.* 231, 482-497.

White, N.M., 2004. The role of stimulus ambiguity and movement in spatial navigation: A multiple memory systems analysis of location discrimination. Neurobiol. Learn. Mem. 82, 216-229.

Figure legends

Fig. 1. Performance of Me5-lesioned and sham-operated mice in the hidden-platform version of the Morris water maze task. (A) Hidden platform test. The time required to reach the hidden platform for sham-operated (n = 8) and Me5-lesioned mice (n = 12) is indicated (mean ± SEM). The mice received four trials on each day over the 5 testing days. Both sham-operated and Me5-lesioned mice showed significant improvement in mean escape latency during the training days (Friedman test, $p < 0.01$; Dunnett *post hoc* comparisons with escape latency, $^{+}p < 0.05$ and $*p < 0.01$ vs. the first day for sham-operated mice; one-way repeated-measures ANOVA followed by *post hoc* Tukey-Kramer tests, $^{+}p < 0.05$ and $*p < 0.01$ vs. the first day for Me5-lesioned mice), and there was no significant difference between the groups. (B) The probe test was performed after the final acquisition trial of the hidden platform test on day 5. Times spent in each of the four quadrants of the pool are shown (mean ± SD). Quadrants are T (target), right, O (opposite to target) and left. Sham-operated and Me5-lesioned mice spent significantly more time in the T than the other three and two quadrants, respectively (one-way repeated-measures ANOVA followed by *post hoc* Tukey-Kramer tests, $^{+}p < 0.05$, $*p < 0.01$ vs. the T).

Fig. 2. Performance of Me5-lesioned and sham-operated mice in the reversal platform version of the Morris water maze task. (A) Reversal platform test. On the day after the hidden-platform test, the hidden platform was switched to the opposite quadrant for reversal training. The mice received four trials on each day over the 2 testing days. The time required to reach the hidden platform for sham-operated (n = 8) and Me5-lesioned mice (n = 12) is indicated (mean ± SEM). Sham-operated but not Me5-lesioned mice showed significant improvement in mean escape latency during the 2 training days (paired *t* test, $^{a}p < 0.01$ vs. the first day), and there was a significant difference between the groups (Welch's *t* test, $^{b}p < 0.01$ on day 2). (B) The reversal probe test was performed after the final acquisition trial of the reversal platform test. Times spent in each of the four quadrants of the pool are shown (mean ± SD). Quadrants are previous T (previous target using the hidden platform test), right, new T (new target) and left. Sham-operated mice spent significantly more time in the new T than the previous T; however, Me5-lesioned mice spent significantly less time in the new T than the previous T (one-way repeated-measures ANOVA followed by *post hoc* Tukey-Kramer tests, $^{+}p < 0.05$ and $*p < 0.01$ vs. the new T).

Fig. 3. Performance of Me5-lesioned and sham-operated mice in the visible platform version of the Morris water maze task. The position of the platform was signaled by the presence of a white flag (8 x 8 cm) above the platform. The platform position varied among four possible positions, and the mice were tested on a total of four trials with a different starting point on each day over the 2 testing days. The time required to reach the visible platform for sham-operated (n = 8) and Me5-lesioned mice (n = 12) is indicated (mean ± SEM). Sham-operated but not Me5-lesioned mice showed significant improvement in mean escape

latency during the two training days (Wilcoxon signed-ranks test, $^{a}p < 0.01$ vs. the first day), and there was a significant difference between the groups (Student's *t* test, $^{b}p < 0.01$ on day 2).

Fig. 4. Total number of BrdU-labeled cells in the dentate gyrus (DG) in Me5-lesioned and sham-operated mice. (A) Photomicrographs of BrdU-labeled cells in the DG of Me5-lesioned and sham-operated mice. Scale bar, 100 μm. (B) Total number of BrdU-labeled cells in the whole of the dentate gyrus of Me5-lesioned (Me5 lesion; n = 5) and sham-operated (sham; n = 4) mice, 12 h after the last BrdU injection. The number of BrdU-labeled cells in Me5-lesioned mice was significantly higher than that in sham-operated mice (Student's *t* test, $*p < 0.05$). Results represent mean ± SD. (C) Histologic analysis of transverse (a, b, c, d; hematoxylin and eosin staining) and longitudinal (e, f, g, h; Nissl staining) brain sections in Me5-lesioned (a, b, e, f) and sham-operated mice (c, d, g, h). Scale bar, 1 mm (a, c, e g), 100 μm (b, d) and 200 μm (f, h). Arrow and broken line show the area of the electrolytic lesions of Me5.

Fig. 5. Neuronal differentiation of the newborn cells in the dentate gyrus in Me5-lesioned and sham-operated mice. (A) Representative confocal images of cells double-labeled with BrdU (red) and NeuN (green). Some BrdU-positive cells colocalize with NeuN (yellow). Scale bar, 50 μm. (B) Quantitative analysis of neuronal differentiation of newborn cells; the total number of both double- and BrdU-positive cells (left) and the number of double-positive cells shown as a percentage of that of BrdU-positive cells (right) were indicated. The number of BrdU-labeled cells that expressed NeuN was estimated by counting these cells from five sections of each mouse. These sections comprised every third section of a series of 13 sections (40 μm thick sections) from the dentate gyrus (1.82 – 2.34 mm posterior to the bregma). The number of both double- and BrdU-labeled cells in Me5-lesioned mice was significantly higher than that in

sham-operated mice (Student's *t* test, [a]$p < 0.01$ vs. BrdU-positive cells in sham-operated mice, [b]$p < 0.01$, [c]$p < 0.01$ vs. double-positive cells in sham-operated mice). Results are presented as mean ± SD.

Fig. 6. The percentage of the newborn cells in the dentate gyrus in Me5-lesioned and sham-operated mice that differentiate into astrocytes, a subclass of glial cells. (A) Representative confocal images of cells double-labeled with BrdU (green) and GFAP (magenta). Some BrdU-positive cells colocalize with GFAP (white). Scale bar, 50 μm. (B) Quantitative analysis of neuronal differentiation of newborn cells; the total number of both double- and BrdU-positive cells (left) and the number of double-positive cells shown as a percentage of that of BrdU-positive cells (right) were indicated. The number of BrdU-labeled cells that expressed GFAP was estimated by counting these cells from five sections of each mouse. These sections comprised every third section of a series of 13 sections (40 μm thick sections) from the dentate gyrus (1.82 – 2.34 mm posterior to the bregma). The percentage of double-labeled cells in Me5-lesioned mice was significantly lower than that in sham-operated mice (Student's *t* test, [a]$p < 0.01$ vs. BrdU-positive cells in sham-operated mice, [b]$p < 0.05$ vs. double-positive cells in sham-operated mice). Results are presented as mean ± SD.

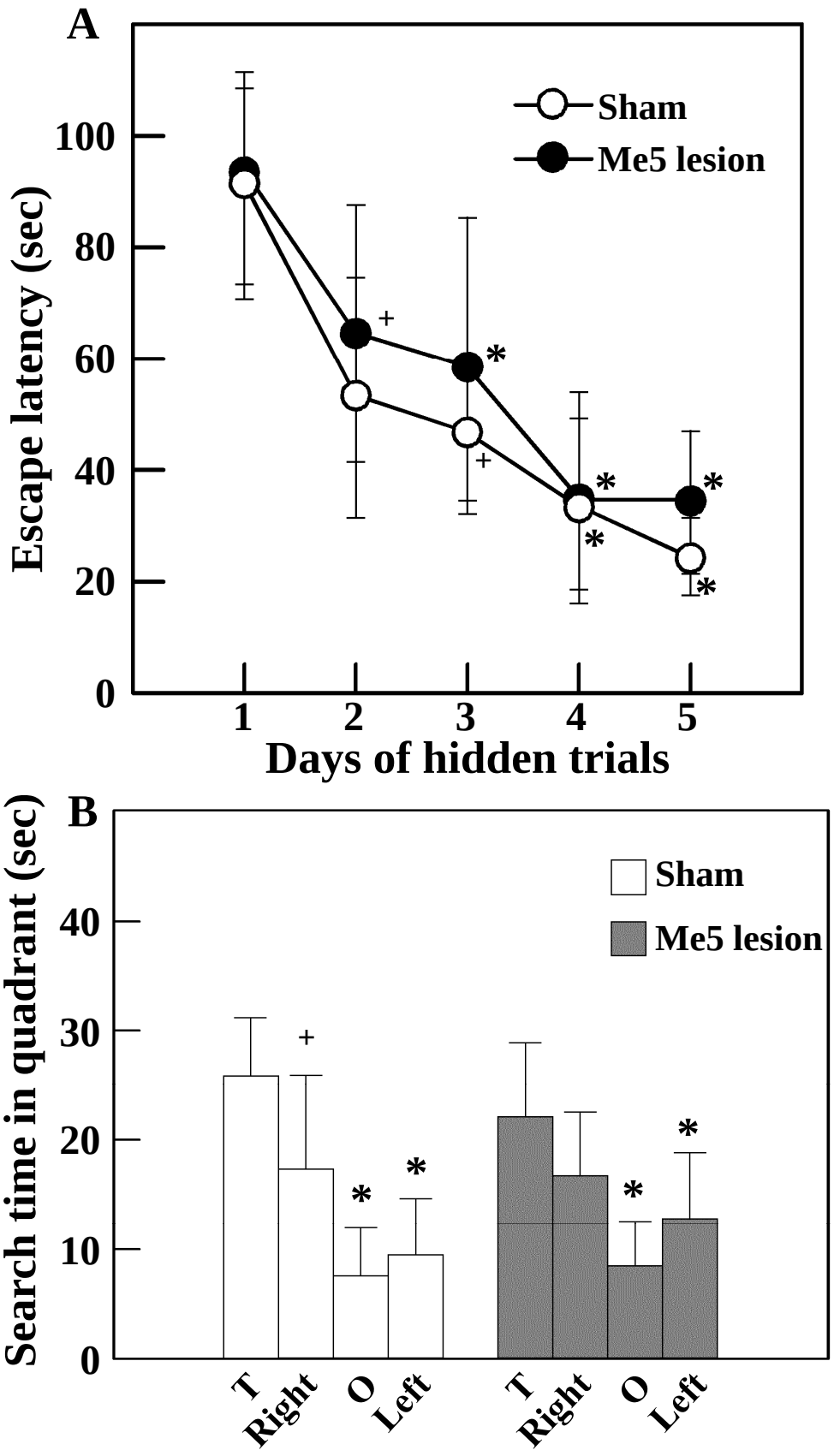
A
Sham
Me5 lesion
Escape latency (sec)
100
80
60
40
20
0
1
2
3
4
5
Days of hidden trials
B
Sham
Me5 lesion
Search time in quadrant (sec)
40
30
20
10
0
T
Right
O
Left
T
Right
O
Left

Fig.1

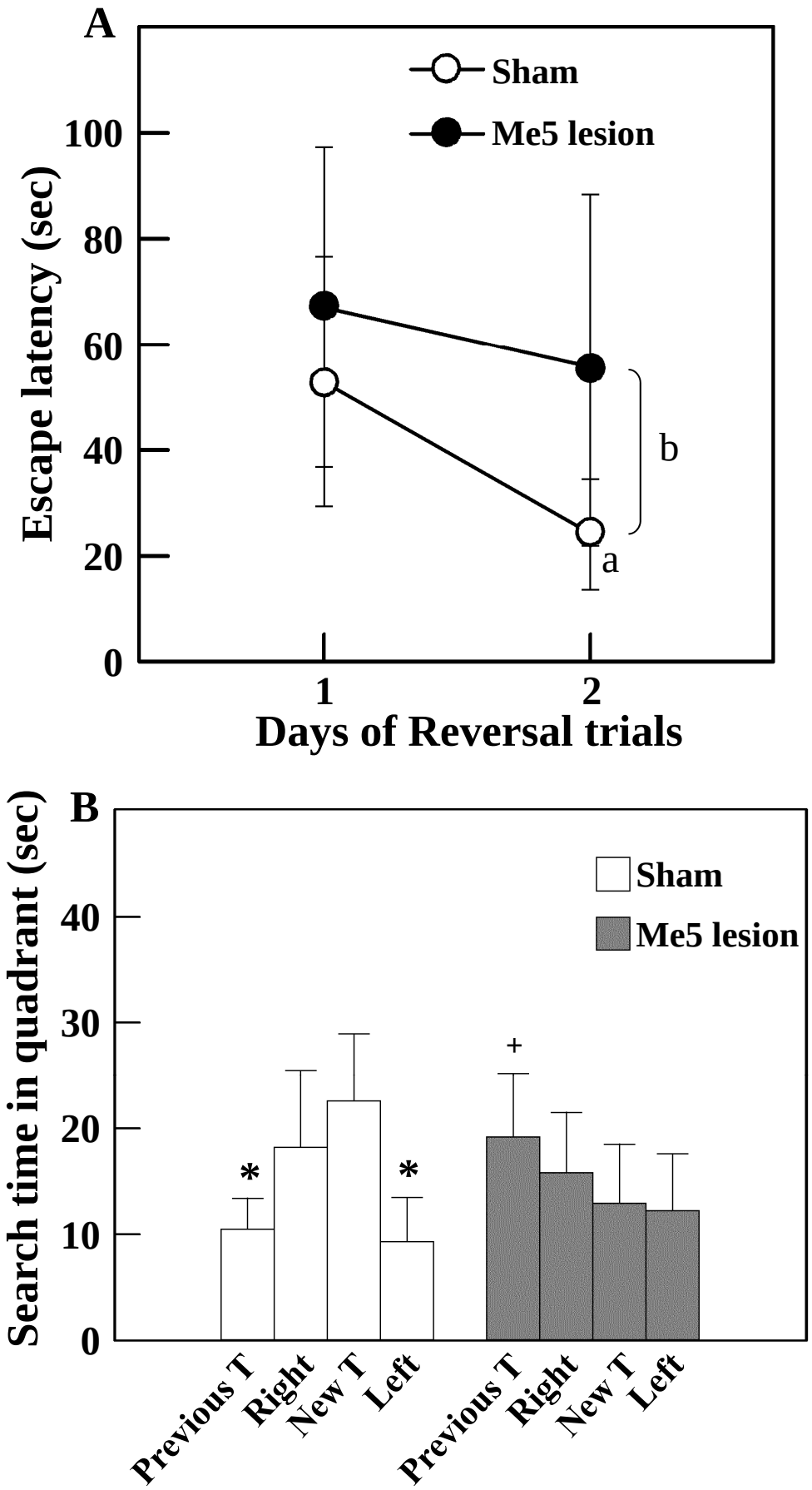
A
Sham
Me5 lesion
Escape latency (sec)
100
80
60
40
20
0
b
a
1
2
Days of Reversal trials
B
Sham
Me5 lesion
Search time in quadrant (sec)
40
30
20
10
0
*
*
+
Previous T
Right
New T
Left
Previous T
Right
New T
Left

Fig.2

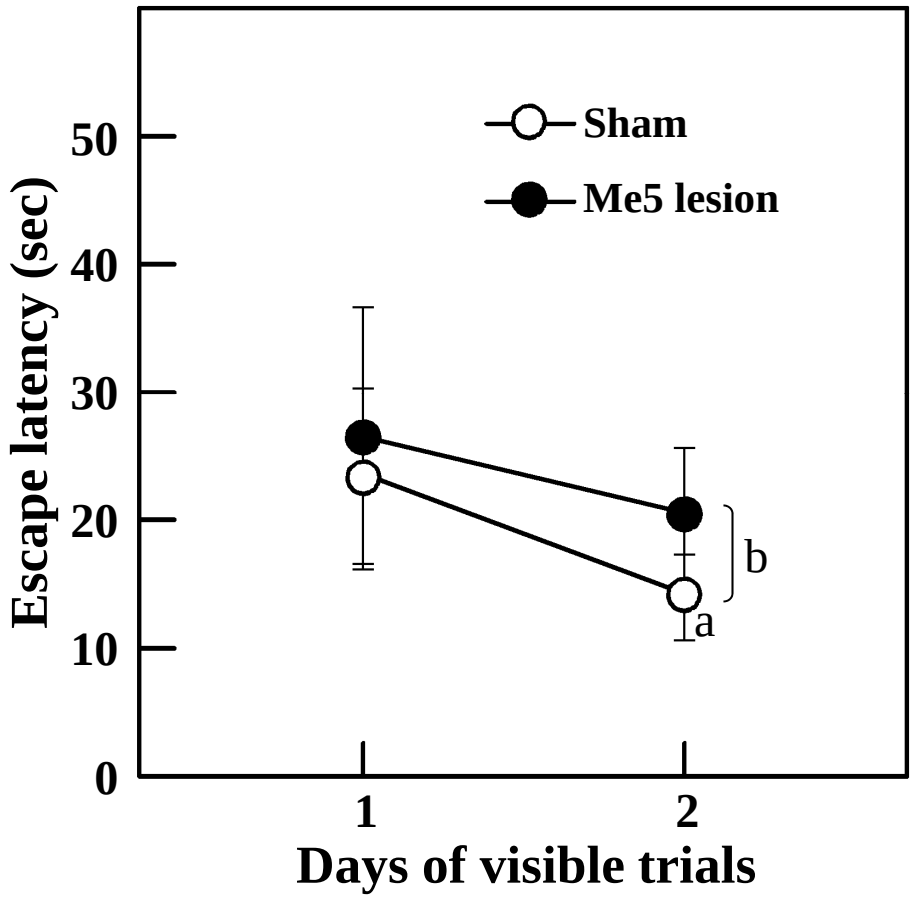
Sham
Me5 lesion
Escape latency (sec)
50
40
30
20
10
0
b
a
1
2
Days of visible trials

Fig.3

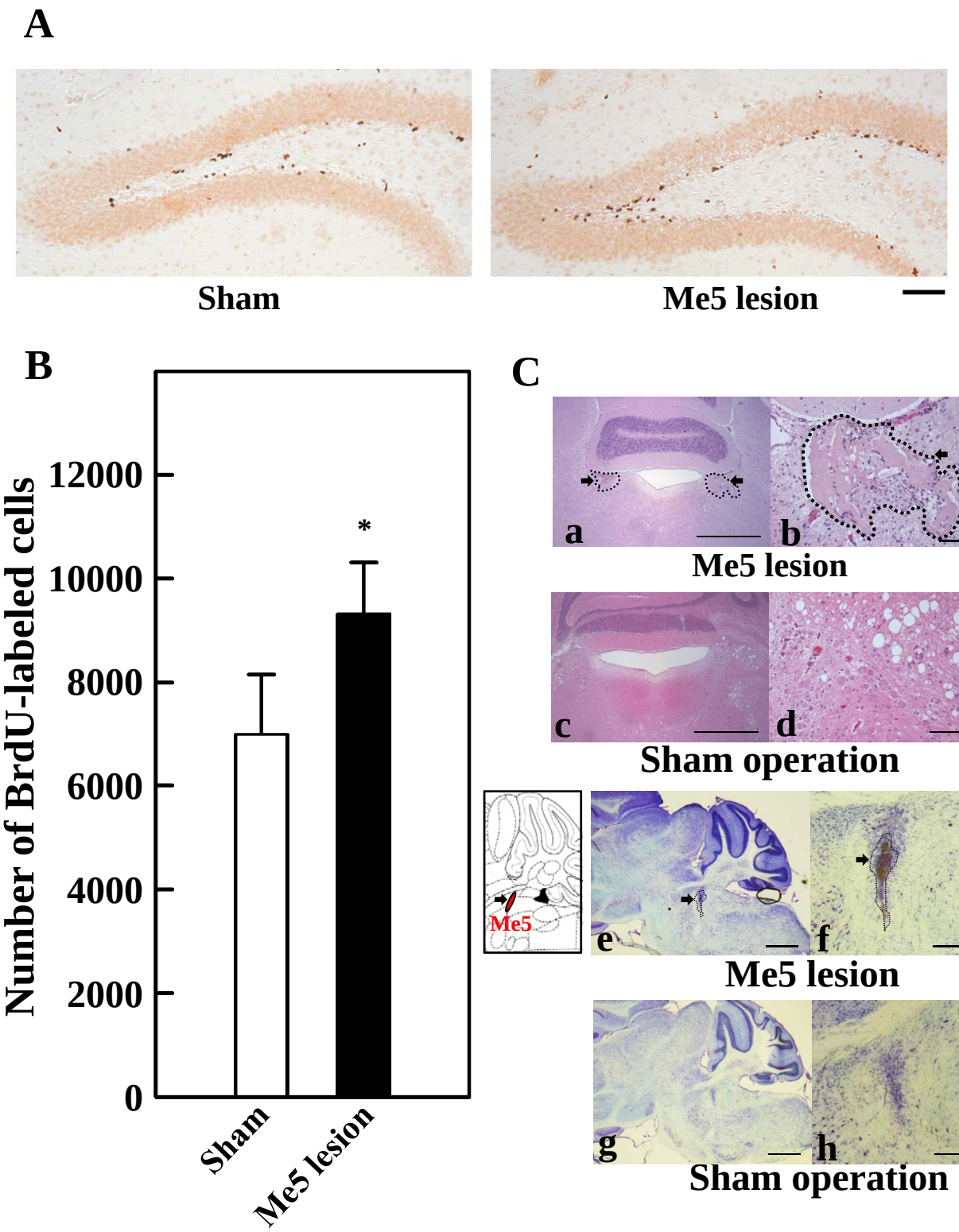
A
Sham
Me5 lesion
B
Number of BrdU-labeled cells
12000
10000
8000
6000
4000
2000
0
*
Sham
Me5 lesion
C
a
b
Me5 lesion
c
d
Sham operation
Me5
e
f
Me5 lesion
g
h
Sham operation

Fig.4

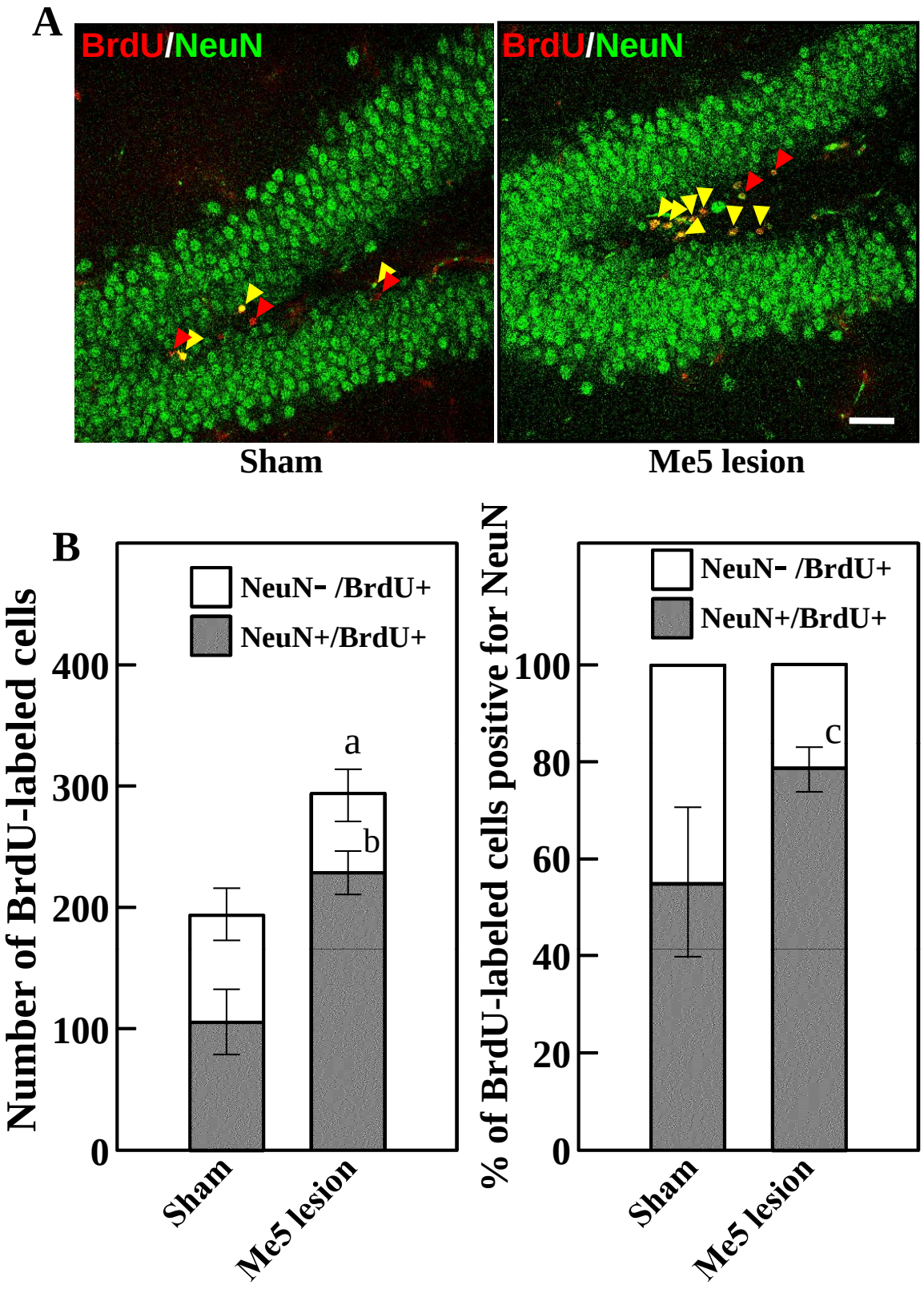
A
BrdU/NeuN
BrdU/NeuN
Sham
Me5 lesion
B
Number of BrdU-labeled cells
NeuN- /BrdU+
NeuN+/BrdU+
400
300
200
100
0
a
b
Sham
Me5 lesion
% of BrdU-labeled cells positive for NeuN
NeuN- /BrdU+
NeuN+/BrdU+
100
80
60
40
20
0
c
Sham
Me5 lesion

Fig.5

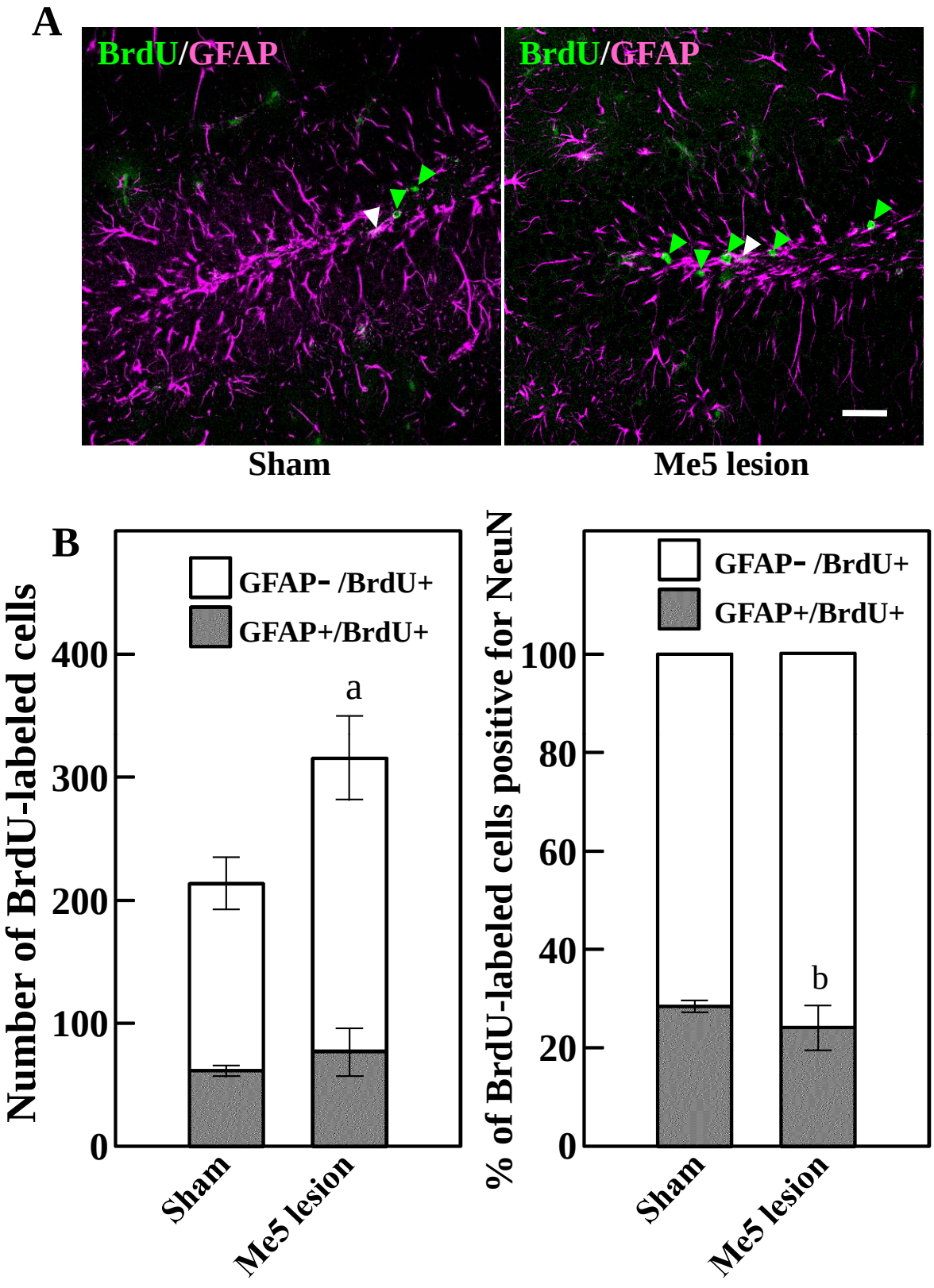
A
BrdU/GFAP
BrdU/GFAP
Sham
Me5 lesion
B
GFAP- /BrdU+
GFAP+/BrdU+
Number of BrdU-labeled cells
400
300
200
100
0
a
Sham
Me5 lesion
GFAP- /BrdU+
GFAP+/BrdU+
% of BrdU-labeled cells positive for NeuN
100
80
60
40
20
0
b
Sham
Me5 lesion

Fig.6

Table 1. Effects of bilateral Me5 lesions on general behavioral activities in the automated hole-board test.

	Locomotion (cm)	**Rearing Counts /Duration (times) / (sec)**	**Head-dip Counts / Duration / Latency (times) / (sec) / (sec)**
Sham operation	**1506.2 ±795.1**	**22.4 ±6.7 / 21.8±12.0**	**23.5 ±8.4 / 16.2±7.0 / 68.6±67.9**
Me5 lesion	**1705.8 ±683.7**	**18.4 ±12.0 / 16.6±12.7**	**20.3 ±10.2 / 11.5±5.6 / 36.2±26.7**

Data are shown as mean±SD.